Similarity Decay of Enstrophy in an Electron Fluid

D. J. Rodgers,[1] W. H. Matthaeus,[1] T. B. Mitchell,[1,*] and D. C. Montgomery[2]
[1]Department of Physics and Astronomy, University of Delaware, Newark, Delaware 19716, USA
[2]Department of Physics and Astronomy, Dartmouth College, Hanover, New Hampshire 03755, USA
(Received 16 May 2010; published 30 November 2010)

A similarity decay law is proposed for enstrophy of a one-signed-vorticity fluid in a circular free-slip domain. It excludes the metastable equilibrium enstrophy which cannot drive turbulence, and approaches Batchelor's t^{-2} law for strong turbulence. Measurements of the decay of a turbulent electron fluid agree well with the predictions of the decay law for a variety of initial conditions.

DOI: 10.1103/PhysRevLett.105.234501 PACS numbers: 47.27.eb, 52.27.Jt, 52.35.Ra

Electron fluids are pure electron plasmas confined within a Malmberg-Penning (MP) trap consisting of hollow conducting cylinders in a uniform axial magnetic field [1]. Electron fluid experiments have garnered attention as a testing ground for 2D turbulence [2], and as a prototype for plasma relaxation [3,4]. The idealized system (neglecting dissipation) is isomorphic to a bounded, singled-signed vortex fluid [5,6]. Substantial effort has been devoted towards understanding the relaxation of a 2D electron fluid towards metastable states that are attained over hydrodynamic time scales [7–11], prior to the much longer decay towards thermal equilibrium. Here we continue the study of the relationship between an electron plasma and 2D hydrodynamics by examining enstrophy decay leading to the metastable equilibrium state, recalling the family of similarity laws for energy decay introduced by Taylor and von Kármán. We find an analogous similarity principle for enstrophy decay, in which the metastable equilibrium enstrophy is set aside as inactive. Experimental measurements agree well with the predictions of this principle for strongly turbulent initial conditions.

A central prediction of statistical turbulence theory [12] is the similarity decay of fluctuation in an incompressible homogeneous turbulent fluid. The ''self-preservation'' hypothesis [13] holds that the velocity autocorrelation function maintains its shape during decay, stretching in response to changes of energy and length scale. Later development [14] described an intermediate (inertial) self-similar range of scales. Later, Kraichnan [15] and Batchelor [16] extended these ideas to 2D turbulence, in which both energy and enstrophy (mean square vorticity) control the nonlinear cascades.

Simulations [17–21] and experiments [22–25] observe a 2D enstrophy cascade, with a wide variation in the observed enstrophy spectrum [26,27]. Batchelor's predicted enstrophy decay law has been more elusive. This difficulty is partially due to the appearance of quasi-isolated vortices [28,29], and at later times, a metastable equilibrium [7–11]. We show that a similarity decay of enstrophy can be obtained once this equilibrium is taken into account. This similarity decay is shown to be valid for a variety of initial conditions with strong nonlinearity without regard for details of the evolution.

Electron fluid experiments are operated in a regime where confinement end effects are minimized and fast motions in the axial direction average over axial variations. As a consequence, to a good approximation the electron density $n(r, \theta, t)$ in these experiments follows 2D, z-averaged, $E \times B$ drift motion [6], with drift velocity

$$\boldsymbol{v}_D = -\frac{c\boldsymbol{\nabla}\phi \times \hat{\boldsymbol{z}}}{B}, \qquad \boldsymbol{\nabla}^2\phi = -4\pi|e|n, \tag{1}$$

where ϕ is the electrostatic potential, B is a uniform magnetic field, and $\boldsymbol{E} = -\boldsymbol{\nabla}\phi$. For this system, $\boldsymbol{v}_D$ is equivalent to the 2D fluid velocity $\boldsymbol{v}$, with the fluid vorticity $\omega = 4\pi|e|cn/B$, and stream function $\psi = -c\phi/B$. With this analogy, we examine the enstrophy decay of a 2D fluid with single-signed vorticity bounded in a circular domain with free-slip boundary conditions.

The 2D vorticity Navier-Stokes (NS) equation is

$$\frac{\partial\omega}{\partial t} + (\boldsymbol{v}\cdot\boldsymbol{\nabla})\omega = \nu\boldsymbol{\nabla}^2\omega, \tag{2}$$

where $\boldsymbol{v}$ is the velocity field with $\omega = \boldsymbol{\nabla}\times\boldsymbol{v}\cdot\hat{\boldsymbol{z}}$ and ν is the kinematic viscosity. Incompressibility requires that $\boldsymbol{v} = \boldsymbol{\nabla}\psi\times\hat{\boldsymbol{z}}$ for a stream function ψ, where $\boldsymbol{\nabla}^2\psi = -\omega$. We choose a bounded circular domain of radius R with free-slip boundary conditions to make correspondence with the MP experiment; then ψ vanishes at radius $r = R$. In the ideal limit $\nu \to 0$, we expect conservation of circulation $C = \langle\omega\rangle$, energy $E = \langle\omega\psi\rangle/2$, and fluid angular momentum $M = \langle 2\psi\rangle$. (The also-conserved central vorticity moment $L = \langle r^2\omega\rangle = CR^2 - 2M$ is sometimes called ''angular momentum'' in MP trap literature.) The fragile invariant enstrophy $\Omega = \langle\omega^2\rangle/2$ may decay through dissipation at the smallest scales.

Electron fluids are neither exactly 2D nor described (in any obvious way) by a simple viscosity ν. Both the physical mechanisms and the functional form of the dissipation mechanisms are expected to differ in NS and electron fluids [30]. Furthermore, the free-slip boundary condition is, in the NS context, at odds with viscous flow. However,

in the electron fluid context, it seems a natural boundary condition, in that it corresponds to a normal electric field at a perfect conductor. Theory incorporating the 2D, inviscid, and free-slip boundary approximations describes reasonably well the global evolution of the 2D electron fluid in the turbulent decay phase [11].

In some cases the electron fluid evolves towards a long-lived metastable state that has considerable spatial nonuniformity. For example, with specially regulated initial conditions, off-axis [31] and "vortex crystal" [32,33] states can be found. However, typically the system evolves rapidly (tens of μs) towards axisymmetry, a property unique to the circular domain. (Subsequent evolution to thermal equilibrium occurs in seconds.) Axisymmetrization assists in suppressing the nonlinearity in Eq. (2), eventually leading to an axisymmetric metastable vorticity $\omega_{\rm ms}$, with a monotonically decreasing radial profile. This state has been analyzed using the conserved quantities and statistical theory [2,34–36] and has been found with reasonable accuracy to agree with experiment [11].

On this basis we postulate that enstrophy of the metastable equilibrium $\Omega_{\rm ms}$ is not available to drive the turbulent dynamics at any time. Accordingly, we define

$$\Omega^F(t) = \Omega(t) - \Omega_{\rm ms}, \tag{3}$$

and call Ω^F the "free enstrophy." The similarity decay of the free enstrophy will take the form

$$\frac{d\Omega^F}{dt} = -a\frac{\Omega^F}{\tau}, \tag{4}$$

where $\tau = \tau(t)$ is the time scale associated with the turbulent decay and a is a constant parameter.

von Kármán's development is based on two point correlation functions in 3D isotropic turbulence [37]. However, inhomogeneity and boundedness of the electron system complicate the study of correlations, so we presume a similarity decay at the onset. The key step is assuming the global time scale τ can depend only on Ω^F and a characteristic length scale l, i.e., $\tau \sim (\Omega^F)^p(l)^q$ for some p, q. The only dimensionally consistent choice is $p = -1/2$, $q = 0$, or $\tau = 1/\sqrt{\Omega^F}$. This is analogous to $\tau = l/\sqrt{E}$ in 3D, where l is a correlation length. Equation (4) becomes $d\Omega^F/dt = -a\Omega^{F(3/2)}$, for which the solution is

$$\frac{\Omega^F}{\Omega_0^F} = [1 + 2a\sqrt{\Omega_0^F}(t - t_0)]^{-2}, \tag{5}$$

where $\Omega_0^F = \Omega^F(t_0)$ is the initial free enstrophy. For an initially disordered fluid with large Ω_0^F, Eq. (5) gives $\Omega^F \sim t^{-2}$ for $a\sqrt{\Omega_0^F}t \gg 1$, as in the isotropic case predicted by Batchelor [16]. The conditions for turbulence to be of sufficient strength to justify a similarity law such as Eq. (4) are not entirely clear, although large $\Omega_0^F/\Omega_{\rm ms}^F$ would seem favorable. This similarity decay of free enstrophy differs from other measures of decay such as one-point measurements of vorticity nonaxisymmetry [9] or coherent-vortex scaling theory [38]. Whereas the latter theories require detailed analysis of dynamic structures of the flow, the similarity decay is a global phenomenology lending itself to a broader class of flows.

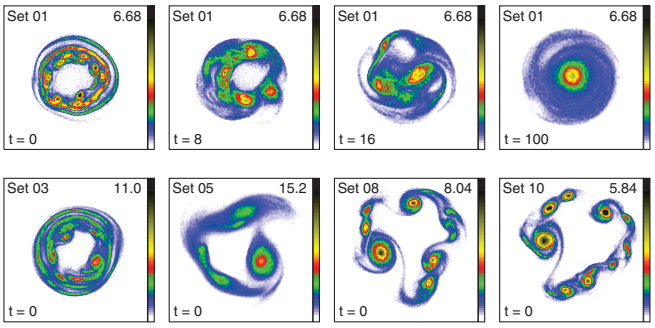

FIG. 1 (color). Top row: Vorticity images showing evolution of data set 01. Bottom: Initial vorticity in four other data sets. Time (μs) and peak vorticity (upper right, μs^{-1}) are shown. Images cropped to one-half the trap radius.

We test this hypothesis by employing data from the University of Delaware MP trap [39,40]. Electrons of temperature $T \simeq 2$ eV are confined inside a series of conducting rings of radius $R = 2.88$ cm and confinement length $L_c = 36.0$ cm. A uniform axial magnetic field $B = 454$ G provides radial confinement. Voltages of $V_c = -80$ V applied to end gate rings provide axial confinement. The rapid axial bounce motion of electrons suppresses axial variations, allowing a 2D $E \times B$ guiding-center drift description. Destructive measurements of electron density involve lowering an end gate, allowing the electrons to stream onto a CCD camera at one end of the chamber; a time series of images is constructed by holding the plasma for successively longer times.

The electron source was a spiral tungsten filament. The filament voltage and the time during which the nearest end gate was lowered (~ 1 μs) were adjusted to produce initial conditions which reflect the structure of the spiral filament; this "streaming" of electrons into the trap without manipulation (via application of external fields) yields sufficient spatial complexity to support turbulence. In such

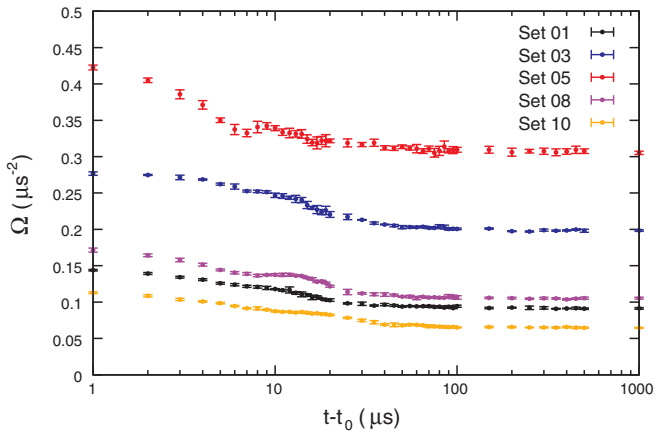

FIG. 2 (color). Enstrophy versus time for the data sets in Fig. 1.

TABLE I. Experimental and fit parameters. Ω has units μs^{-2}. Best-fit parameter is a [Eq. (5)]; χ^2 ($\times 10^{-3}$) is mean-squared difference of data and best-fit curve. Last three data sets are hollow initial conditions as in [8,9].

Set	01	02	03	04	05	06	07	08	09	10	11	12	13	14	15	16	17
Ω_0	0.290	0.423	0.569	0.772	0.867	0.740	0.620	0.359	0.298	0.234	0.115	0.418	0.375	0.548	1.04	0.723	0.540
Ω_{ms}	0.183	0.277	0.397	0.582	0.610	0.561	0.399	0.211	0.172	0.129	0.059	0.284	0.218	0.382	0.939	0.620	0.428
a	0.086	0.100	0.052	0.034	0.101	0.101	0.058	0.074	0.082	0.077	0.149	0.030	0.032	0.043	0.016	0.010	0.008
χ^2_a	0.573	0.417	1.37	1.67	2.29	1.02	1.48	2.57	1.29	1.78	1.10	3.04	1.87	2.68	7.98	4.29	13.0

cases the dynamics are characterized by many vorticies and long filaments that interact and merge, leading to the axisymmetric metastable state ω_{ms} [11]. An example of this evolution is shown in the top row of Fig. 1; the bottom row shows initial conditions for four other data sets. The corresponding enstrophy decay curves are shown in Fig. 2. Table I shows Ω_0 and Ω_{ms} for these five data sets (as well as for data sets discussed later). Also analyzed are axisymmetric "hollowed" initial conditions, where a bulk column of charge in near-thermal equilibrium is hollowed out to various depths. This initial condition is nonturbulent, but subject to the Kelvin-Helmholtz instability [8,9]. The linear instability grows, leading eventually to an axisymmetric state, but although enstrophy decreases, it is unclear if the evolution becomes strongly turbulent.

We begin by analyzing the streamed data set 01 shown in Fig. 1. The metastable state ω_{ms} is identified with the experimental state at 1000 μs, and Ω_{ms} is defined using ω_{ms}. Note that 1000 μs is not so late that nonfluid-like dissipative effects emerge [41], or that thermal equilibrium is attained. This final time is used for all data sets. For hollowed data sets, t_0 is chosen at the onset of the decay phase (~ 100 μs); all others have $t_0 = 0$.

Comparing the free enstrophy Ω^F and the prediction in Eq. (5), we find the parameter a that produces the best least-squares fit. Figure 3(a) shows this comparison for data set 01. The similarity decay law fits the data very well, with a mean-squared error of $\chi^2 \approx 6 \times 10^{-4}$.

We carried out similar procedures on 16 other data sets, the last three starting from hollowed profiles. Despite the variety of the initial conditions, most of these data sets are fit well by Eq. (5), although the hollowed initial conditions deviate significantly. To show this, we first plot Ω^F/Ω_0^F versus the experimental time $t - t_0$ in Fig. 3(b). The curves clearly display some similarity, but the best fits to Eq. (5) have different values of a; see Table I. However, when Ω^F/Ω_0^F is plotted against the adjusted nonlinear time $a\sqrt{\Omega_0^F}(t - t_0)$, all the curves collapse onto a single decay curve, as shown in Fig. 3(c).

The best-fit parameters of these five data sets have an average $a \approx 0.1$. Evidently the reciprocal global decay time τ overestimates the magnitude of the relaxation rate. Intuitively, this seems related to suppression of nonlinearity associated with the emergence of near isolated vortices and near-axisymmetric states [17,18,28,42], analogous to the nonlinear suppression due to Beltrami flows in 3D turbulence [43]. This is qualitatively verified by observing the five data sets in Fig. 1 ordered by decreasing a (05, 01, 10, 08, 03); this sequence also gives roughly the order for increasing level of vorticity localization *or* increasing level of global axisymmetry. This relationship is also seen in the other data sets.

As a final demonstration, the free enstrophy decay prediction, Eq. (5), is rearranged to have a linear dependence on the nonlinear time $\sqrt{\Omega_0^F}(t - t_0)$, and the experimental values of all available data sets are used to scatter plot the (inverse) left-hand side versus the right-hand side in Fig. 4. Here we do not optimize the parameter a, as in Fig. 3, but instead we use the value of $a = 0.1$. The streamed data sets follow the similarity prediction for 2 orders of magnitude of $\sqrt{\Omega_0^F}(t - t_0)$. Only the hollowed profiles (top three traces) deviate significantly from the trend line, and for these, the theory may be inapplicable due to insufficient turbulence strength [10]. For the fully turbulent cases, a

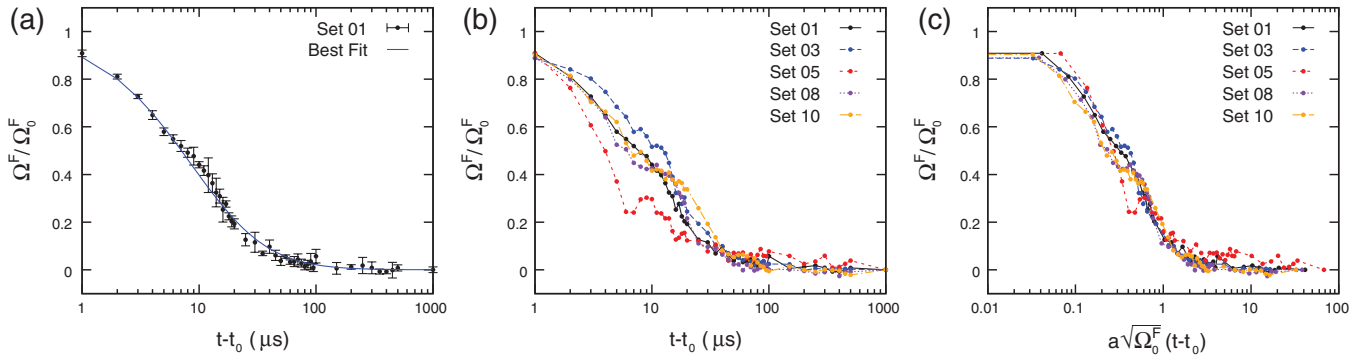

FIG. 3 (color). Scaled free enstrophy versus (a),(b) experimental time and (c) adjusted nonlinear time. Panel (a) shows the data set 01 and best fit to Eq. (5), (b) and (c) show all data sets from Fig. 2.

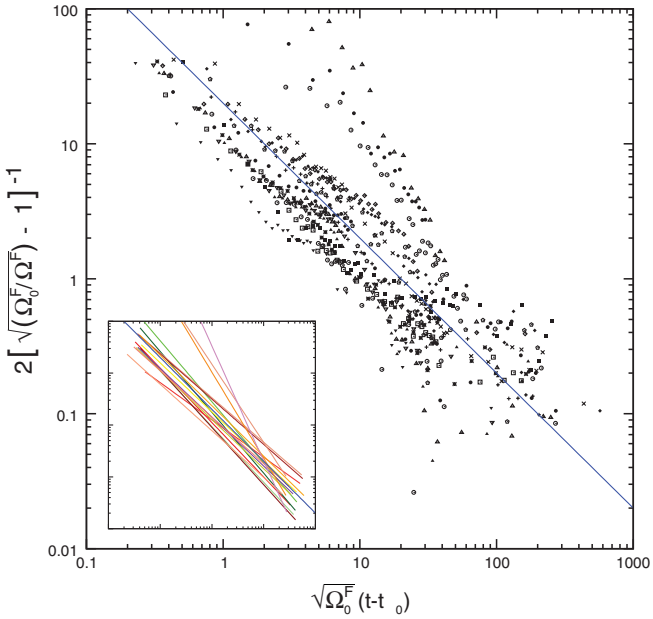

FIG. 4 (color). Free enstrophy series for all data sets in Table I; blue line is $a = 0.1$. Inset: Data sets fit to $[a_\lambda \sqrt{\Omega_0^F}(t - t_0)]^{-\lambda}$.

reasonable accounting of the rapid period of enstrophy decay is provided in this simple theory, without any discussion of details of the flow.

We suggest several conclusions. First, in defining the direct enstrophy cascade time scale, it is apparently reasonable to separate from the total enstrophy the fraction that is destined to be associated with the ''most probable'' quasiequilibrium state attained after many characteristic dynamical times. This makes it possible to employ a von Kármán-like similarity analysis even without a very large initial enstrophy. When the initial enstrophy is large, the proposed model exhibits a self-similar decay of enstrophy which mirrors Batchelor's t^{-2} law. Second, experimental evidence in the small initial enstrophy regime points to validity of this similarity decay for a variety of initial conditions. The results appear to depend on both the initial degree of vorticity localization and the amount of global axisymmetry of the initial conditions. This may be useful in guiding future refinements of the phenomenology. Finally, the successes of the hydrodynamic phenomenology in describing 2D electron dynamics continue to accrue. So far, serious discrepancies between 2D relaxation in electron fluids and hydrodynamics have not emerged. Future work may find it useful to explore the limits of the analogy between $E \times B$ drift Penning trap dynamics and 2D hydrodynamic turbulence by examining and comparing higher Reynolds number behavior, employing a wider variety of experimental results, and comparing higher order statistical quantities in the two cases. In addition, the theoretical understanding of the source of kinetic dissipation in the electron trap plasma remains a wide open topic.

This research supported in part by DOE Grant No. DE-FG02-06ER54853, and by NSF ATM-0539995.

*Present address: 103 Cornell Avenue, Swarthmore, PA 19081, USA.

[1] T. B. Mitchell and C. F. Driscoll, Phys. Fluids **8**, 1828 (1996).
[2] D. Montgomery and G. Joyce, Phys. Fluids **17**, 1139 (1974).
[3] J. B. Taylor, Phys. Rev. Lett. **33**, 1139 (1974).
[4] R. H. Kraichnan and D. Montgomery, Rep. Prog. Phys. **43**, 547 (1980).
[5] R. J. Briggs *et al.*, Phys. Fluids **13**, 421 (1970).
[6] C. F. Driscoll and K. S. Fine, Phys. Fluids B **2**, 1359 (1990).
[7] D. Montgomery *et al.*, Phys. Fluids A **4**, 3 (1992).
[8] X. Huang and C. F. Driscoll, Phys. Rev. Lett. **72**, 2187 (1994).
[9] X.-P. Huang *et al.*, Phys. Rev. Lett. **74**, 4424 (1995).
[10] H. Brands *et al.*, Phys. Fluids **11**, 3465 (1999).
[11] D. J. Rodgers *et al.*, Phys. Rev. Lett. **102**, 244501 (2009).
[12] G. I. Taylor, Proc. R. Soc. A **151**, 421 (1935).
[13] T. de Karman and L. Howarth, Proc. R. Soc. A **164**, 192 (1938).
[14] A. Kolmogorov, Dokl. Akad. Nauk SSSR **30**, 301 (1941) [republished in Proc. R. Soc. A **434**, 9 (1991)].
[15] R. H. Kraichnan, Phys. Fluids **10**, 1417 (1967).
[16] G. K. Batchelor, Phys. Fluids **12**, II-233 (1969).
[17] R. Benzi *et al.*, J. Phys. A **21**, 1221 (1988).
[18] W. H. Matthaeus *et al.*, Physica (Amsterdam) **51D**, 531 (1991).
[19] V. Borue, Phys. Rev. Lett. **71**, 3967 (1993).
[20] J. J. Rasmussen *et al.*, Phys. Scr. **T98**, 29 (2001).
[21] D. Montgomery *et al.*, Phys. Fluids A **5**, 2207 (1993).
[22] A. Belmonte *et al.*, Phys. Fluids **11**, 1196 (1999).
[23] Y. Kawai *et al.*, Phys. Rev. E **75**, 066404 (2007).
[24] J. Paret *et al.*, Phys. Rev. Lett. **83**, 3418 (1999).
[25] S. Danilov *et al.*, Phys. Rev. E **65**, 036316 (2002).
[26] R. H. Kraichnan, J. Fluid Mech. **47**, 525 (1971).
[27] B. K. Shivamoggi, J. Phys. A **23**, 1689 (1990).
[28] J. C. McWilliams, J. Fluid Mech. **146**, 21 (1984).
[29] W. H. Matthaeus *et al.*, Phys. Rev. Lett. **66**, 2731 (1991).
[30] J. M. Kriesel and C. F. Driscoll, Phys. Rev. Lett. **87**, 135003 (2001).
[31] E. Sarid *et al.*, Phys. Rev. Lett. **93**, 215002 (2004).
[32] K. S. Fine *et al.*, Phys. Rev. Lett. **75**, 3277 (1995).
[33] D. Durkin and J. Fajans, Phys. Fluids **12**, 289 (2000).
[34] J. H. Williamson, J. Plasma Phys. **17**, 85 (1977).
[35] D. Montgomery *et al.*, J. Plasma Phys. **21**, 239 (1979).
[36] D. Montgomery *et al.*, Phys. Fluids **21**, 757 (1978).
[37] W. H. Matthaeus *et al.*, J. Plasma Phys. **56**, 659 (1996).
[38] G. F. Carnevale *et al.*, Phys. Fluids A **4**, 1314 (1992).
[39] T. B. Mitchell *et al.*, in *Non-Neutral Plasmas VI*, AIP Conf. Proc. No. 862 (AIP, New York, 2006), pp. 29–38.
[40] N. Mattor *et al.*, Phys. Rev. Lett. **96**, 045003 (2006).
[41] C. F. Driscoll *et al.*, Phys. Fluids **29**, 2015 (1986).
[42] C.-H. Bruneau *et al.*, Europhys. Lett. **78**, 34 002 (2007).
[43] R. H. Kraichnan and R. Panda, Phys. Fluids **31**, 2395 (1988).